

actual experimental nucleation rates are substantially higher than the corresponding theoretical values. In this connection it is particularly important to mention that possible effects due to vapor depletion and production of latent heat by growing droplets during the expansion pulse would cause a reduction of the measured droplet concentrations. Furthermore, these effects would be increasingly important with increasing concentrations. Accordingly, the experimental nucleation rates as well as the slope of the experimental rate vs. supersaturation curves can be considered as lower limits for the "actual" values.

Results of measurements for other systems will be presented later. In addition, a detailed description of our apparatus and a comprehensive presentation of our experimental data in quantitative comparison with theory are in preparation.

Summary and Conclusions

Using a two-piston expansion chamber, we measured homogeneous nucleation rates over a range from $\sim 2 \times 10^5$ to $2 \times 10^9 \text{ cm}^{-3} \text{ s}^{-1}$. For water vapor in argon, homogeneous nucleation rates were measured recently by Miller³⁵ and Anderson et al.³⁹ using a one-piston expansion chamber. As can be seen in Figure 5, their data^{35,39} together with our results cover a range of as much as 8 orders of magnitude. In the narrow range of overlap, an agreement within a factor of ~ 2 is observed. In the experiments^{35,39} nucleation pulse durations of ≥ 10 ms were considered, whereas we obtained sensitive times of ~ 1 ms. In order to achieve the required fast pressure changes, the measuring chamber had to be chosen much smaller than in ref 35 and 39. We determined the droplet number concentration by meas-

uring the scattered-light flux as a function of time during nucleation and droplet growth. A different detection technique was applied in ref 35 and 39. In view of these differences, the above-mentioned agreement appears to be quite good and supports the data^{35,39} as well as our results.

A comparison with the classical nucleation theory shows that the experimental nucleation rates for water-argon (Figure 5) are smaller than the theoretical values, the disagreement becoming more pronounced at higher supersaturations and nucleation rates. Accordingly, for some lower value of the nucleation rate, agreement between experiment and theory could be expected. Actually, diffusion-chamber experiments^{19,21,36,37} show that the classical nucleation theory "provides a fair approximation to the experimental results"²¹ for nucleation rates of the order of $1 \text{ cm}^{-3} \text{ s}^{-1}$. The results^{35,39} and our data indicate that for the system water-argon this agreement is limited to small nucleation rates. While for water-argon we measured nucleation rates smaller than predicted by the Becker-Döring theory, the opposite was found for 1-propanol vapor in nitrogen (Figure 6). These results seem to be consistent with Abraham's³⁸ conclusion that "the apparent success of the Becker-Döring theory to predict the nucleation of polar liquids is believed to be fortuitous".

Acknowledgment. This work was performed in the department of Professor Dr. M. Kahlweit. We thank him for the support of this work and for many helpful discussions. P.E.W. received a scholarship from the Max-Planck-Gesellschaft, which is gratefully acknowledged. The light-scattering calculations were performed by W. Szymanski at the University of Vienna.

An FT IR Study of the Isomerization and O₂ Reaction of *n*-Butoxy Radicals

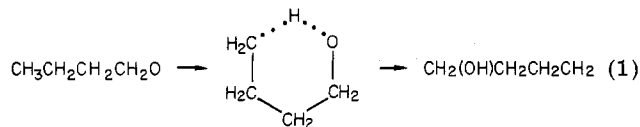
H. Niki,* P. D. Maker, C. M. Savage, and L. P. Breitenbach

Engineering and Research Staff, Research, Ford Motor Company, Dearborn, Michigan 48121 (Received: April 23, 1981; In Final Form: June 5, 1981)

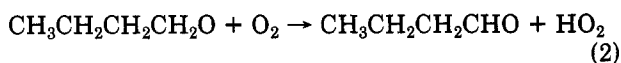
Using the long path FT IR method, we made product studies of the photolysis of *n*-butyl nitrite ($n\text{-C}_4\text{H}_9\text{ONO}$) in ppm concentrations at 700 torr of air and 298 ± 2 K. Unidentified HO-containing compounds as well as *n*-butyraldehyde ($n\text{-C}_3\text{H}_7\text{CHO}$) were detected. The results provide further evidence for the occurrence of the following competitive uni- and bimolecular reaction paths for the ensuing *n*-butoxy radicals: intramolecular hydrogen-shift isomerization $\text{CH}_3\text{CH}_2\text{CH}_2\text{CH}_2\text{O} \cdot \rightarrow \dot{\text{C}}\text{H}_2\text{CH}_2\text{CH}_2\text{CH}_2\text{OH}$ (1), and O₂ reaction $\text{CH}_3\text{CH}_2\text{CH}_2\text{CH}_2\text{O} \cdot + \text{O}_2 \rightarrow \text{CH}_3\text{CH}_2\text{CH}_2\text{CHO} + \text{HO}_2$ (2). From the observed yield of *n*-C₃H₇CHO, the relative rate $k_2[\text{O}_2]/k_1$ has been determined to be 0.23 ± 0.03 (2σ) at 700 torr of air.

Introduction

As pointed out first by Carter et al.,¹ one of the important kinetic features of atmospheric reactions involving large alkane hydrocarbons ($\geq \text{C}_4$) is the significant occurrence of internal isomerization of the ensuing alkoxy radicals by 1,5-hydrogen shift via a low-strain six-member ring intermediate. This type of unimolecular reaction of alkoxy radicals is well-known in combustion chemistry.² The *n*-butoxy radical is the smallest alkoxy radical that can undergo such isomerization, i.e.



Under standard ambient conditions (STP: 300 K and 700 torr of air) a possible alternative fate of this radical is the intermolecular hydrogen-transfer reaction with O₂, reaction 2. On the basis of thermochemical kinetics, Baldwin et



al.³ and Carter et al.¹ estimated the ratio of (isomeriza-

(1) W. P. L. Carter, K. R. Darnall, A. C. Lloyd, A. M. Winer, and J. N. Pitts, Jr., *Chem. Phys. Lett.*, **42**, 22 (1976).

(2) See, for example, ref 20-30 cited in ref 1.

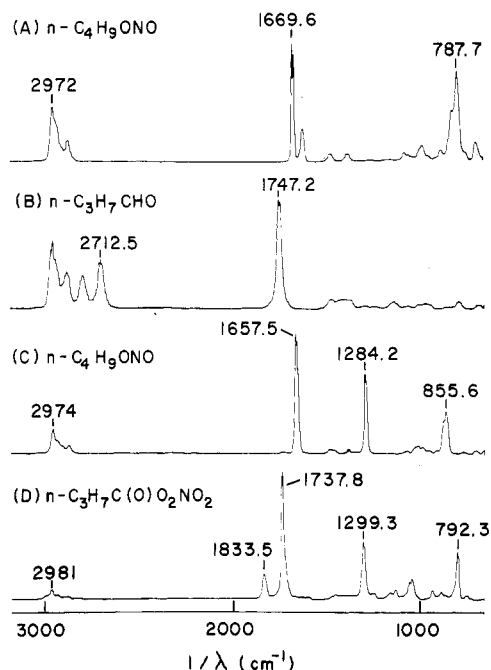


Figure 1. Absorbance spectra of several reference compounds. (A) *n*-C₄H₉ONO [0.5 torr], (B) *n*-C₃H₇CHO [1.0 torr], (C) *n*-C₄H₉ONO₂ [0.68 torr], and (D) *n*-C₃H₇C(O)O₂NO₂ [~0.25 torr]. All the spectra are displayed on an identical absorbance scale. The peak height at 1669.6 cm⁻¹ in (A) corresponds to $\log [I_0/I] = 0.82$.

tion/O₂ reaction), $k_1/k_2[\text{O}_2] = 100\text{--}300$ with an uncertainty of a factor of ~100. More recently, Carter et al.⁴ obtained an experimental value of 3.4 for this rate ratio in a smog chamber study of *n*-butane-NO_x mixtures in ppm concentrations at 735 torr of air and 303 K. Thus, the role of reactions 1 and 2 should be considered under atmospheric conditions.

The present study was undertaken in an attempt to determine the relative importance of reactions 1 and 2 in a somewhat more direct fashion, and also to obtain spectroscopic evidence for the formation of HO-containing products formed in the subsequent reactions of the CH₂(OH)CH₂CH₂CH₂ radicals. For this purpose, *n*-butoxy radicals were generated directly by the photodissociation of *n*-butyl nitrite and product analyses were made over a range of experimental parameters, e.g., reactant conversion, O₂ pressure, and addition of "HO-radical scavengers".

Experimental Section

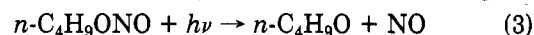
Photooxidation of *n*-C₄H₉ONO was carried out in a 3-m long Pyrex IR cell (180-m folded path), and products were analyzed by using the FT IR spectroscopic method. Details of the facility and its performance characteristics have been described previously.⁵ Typical absorbance spectra shown in this paper were recorded in 1.5 min (16 scans) at $\Delta\nu = 1/16$ cm⁻¹. UV fluorescent lamps (GE F40 BLB) were used for the irradiation. The photolytic intensity corresponded typically to an observed decay lifetime of 10 min for *n*-C₄H₉ONO in ppm concentrations in 700 torr of air.

Shown in Figure 1 are some of the reference spectra used in this study, i.e., the reactant *n*-C₄H₉ONO and possible primary and secondary products *n*-C₃H₇CHO, *n*-

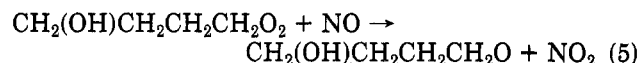
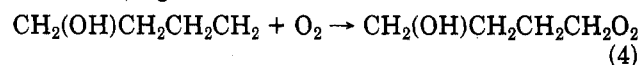
C₄H₉ONO₂, and *n*-C₃H₇C(O)OONO₂. All the spectra were recorded in the presence of 700 torr of air. Frequencies are given for the major, conspicuous absorption bands of these spectra. With the exception of the unstable compound *n*-C₃H₇C(O)OONO₂, the gaseous samples were introduced to a 50-cm long Pyrex cell (1-m folded path) by directly monitoring their partial pressures in the 0.1–1-torr range; *n*-C₃H₇C(O)OONO₂ was prepared in ppm concentrations in the long-path cell by the Cl-atom initiated oxidation of *n*-C₃H₇CHO in the presence of NO₂. Typically, 1 min irradiation of a mixture containing *n*-C₃H₇CHO (5 ppm), NO₂ (5 ppm), and Cl₂ (20 ppm) in 700 torr of air resulted in 40% conversion of the *n*-C₃H₇CHO to virtually pure *n*-C₃H₇C(O)OONO₂. Both *n*-C₄H₉ONO and *n*-C₄H₉ONO₂ were prepared according to well-established methods described in the literature.^{6,7}

Results and Discussion

The photolysis of *n*-C₄H₉ONO in 700 torr of air resulted in a complex product distribution whose major features can be summarized as follows. *n*-C₃H₇CHO was positively identified among the photolytic products by its absorption band centered at 2712.5 cm⁻¹. Its observed yield was approximately 20% of the *n*-C₄H₉ONO consumed. The majority of the remaining *n*-C₄H₉ONO reacted led to the formation of unidentified products as described later in some detail. Among the major nitrogen-containing products were NO₂ and HOONO₂. Qualitatively, these results suggest that the photodissociation of *n*-C₄H₉ONO, reaction 3, was followed by the competitive reactions involving the



ensuing *n*-C₄H₉O radicals, reactions 1 and 2. The observed rapid formation of NO₂ from the primary photolytic product NO appeared to occur primarily in the subsequent oxidation of the CH₂(OH)CH₂CH₂CH₂ radicals formed by reaction 1, e.g.



Reactions subsequent to (5) led to the formation of HO₂ radicals, since the formation of HOONO₂ by reaction 6 persisted even when low O₂ pressure conditions rendered reaction 2 negligible as compared to reaction 1.



Unfortunately, many of the reaction products, particularly HOONO₂ and the unknown products decayed rapidly with a lifetime of 5–10 min, and could not be characterized reliably. Therefore, experiments were conducted to first obtain quantitative data on the *n*-C₃H₇CHO yield from which the relative rate, $k_2[\text{O}_2]/k_1$, for reactions 1 and 2 could be derived by using eq 1, where *Y* is the fractional

$$k_2[\text{O}_2]/k_1 = Y/(1 - Y) \quad (1)$$

yield of *n*-C₃H₇CHO, $\Delta[n\text{-C}_3\text{H}_7\text{CHO}]/\Delta[n\text{-C}_4\text{H}_9\text{ONO}]$. Implicit in eq 1 are two mechanistic assumptions. Namely, the experiment must be designed to minimize possible secondary consumption of both *n*-C₄H₉ONO and *n*-C₃H₇CHO, and to minimize the secondary reactions of the *n*-C₄H₉O radicals, i.e., reactions other than (1) and (2). The potentially important secondary reactions of *n*-C₄H₉ONO

(3) A. C. Baldwin, J. R. Barker, D. M. Golden, and D. G. Hendry, *J. Phys. Chem.*, **81**, 2483 (1977).

(4) W. P. L. Carter, A. C. Lloyd, J. L. Spring, and J. N. Pitts, Jr., *Int. J. Chem. Kinet.*, **11**, 45 (1979).

(5) P. D. Maker, H. Niki, C. M. Savage, and L. P. Breitenbach, *Am. Chem. Soc. Symp. Ser.*, No. 94, 163 (1979).

(6) R. Boschan, R. Merrow, and R. Van Dolah, *Chem. Rev.*, **55**, 485 (1955).

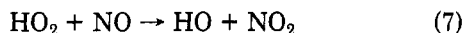
(7) I. O. Sutherland, Ed., "Comprehensive Organic Chemistry", Vol. 2, Pergamon Press, New York, 1978.

TABLE I: Measurements of the Relative Rate $k_2[\text{O}_2]/k_1$ at 700 torr of Air and 298 ± 2 K

$[n\text{-C}_4\text{H}_9\text{-ONO}]_0$, ppm	$[\text{C}_2\text{H}_4]_0$, ppm	$-\text{[}n\text{-C}_4\text{H}_9\text{-ONO] conversion, \%}$	$[\text{C}_3\text{H}_7\text{-CHO}]$ yield, %	$k_2[\text{O}_2]/k_1$
5.4		22.2	19.2	0.24
6.5		30.8	18.2	0.22
10.4		33.7	16.9	0.20
5.1	10	31.4	18.6	0.23
5.2	20	28.6	17.8	0.22
4.9	40	52.4	17.7	0.22
5.4	40	31.2	17.1	0.21
10.2	40	27.2	19.9	0.25
5.8	10 ^a	25.9	19.3	0.24
8.2	10 ^b	28.0	20.0	0.25
				0.23 ± 0.03 (2 σ)

^a C₃H₆ added. ^b NO₂ added.

and $n\text{-C}_3\text{H}_7\text{CHO}$ are those involving HO radicals formed by reaction 7. However, interferences from these reactions



were judged to be minimal because of the dominant occurrence of the series of reactions 1, 5, 6, etc., over reaction 7 at STP. This conclusion was justified by the results of several runs in which the C₃H₇CHO yield was measured and found to be constant in the presence of "HO-radical scavengers" such as C₂H₄ and C₃H₆ at sufficient concentrations. Similarly, the potentially significant interfering reaction of $n\text{-C}_4\text{H}_9\text{O}$ with NO₂ was judged to be of negligible importance with the product NO₂ concentration below a few ppm. The literature value⁸ for the NO₂ reactions of CH₃O radical combined with the rate ratio, $k_2[\text{O}_2]/k_1$, obtained in this study suggest that 10 ppm of NO₂ initially added to the system would consume at most 10% of the $n\text{-C}_4\text{H}_9\text{O}$ radicals formed. This estimate was verified by a run made with 10 ppm of added NO₂. In this run, the observed $n\text{-C}_3\text{H}_7\text{CHO}$ yield did not deviate by more than 10% from an average value obtained without adding NO₂. These results are summarized in Table I. In this table, no trends are discernible for the observed yield of $n\text{-C}_3\text{H}_7\text{CHO}$ and thus for the derived rate ratio, $k_2[\text{O}_2]/k_1$. In addition, the expected dependence of the $n\text{-C}_3\text{H}_7\text{CHO}$ yield on the O₂ pressure was verified over the range of 1–700 torr of O₂. However, the precision and accuracy of these data were judged to be much poorer than those in 700 torr of air and were not included in Table I. Thus, from an average value of $k_2[\text{O}_2]/k_1 = 0.23 \pm 0.02$ (σ) given in this table, the rate constant ratio k_1/k_2 was determined to be $(1.9 \pm 0.2 [\sigma]) \times 10^{19}$ molecule cm⁻³. This value is in excellent agreement with an earlier experimental value of 1.6×10^{19} molecule cm⁻³ obtained by Carter et al.⁴ based on the $n\text{-C}_3\text{H}_7\text{CHO}$ yield in the photooxidation of $n\text{-butane-NO}_x$ mixture. On the other hand, the thermochemical estimate^{1,3} of the rate ratio $k_2[\text{O}_2]/k_1 = 0.003\text{--}0.01$ at STP is less than the experimental values by a factor of about 100, although this should be considered to be within the probable uncertainty. The major source for this discrepancy appears to be in the estimated rate for the isomerization, since the rate constant, for the O₂ reaction of $n\text{-C}_3\text{H}_7\text{O}$ was based on experimental values for analogous reactions involving other alkoxy radicals.⁹

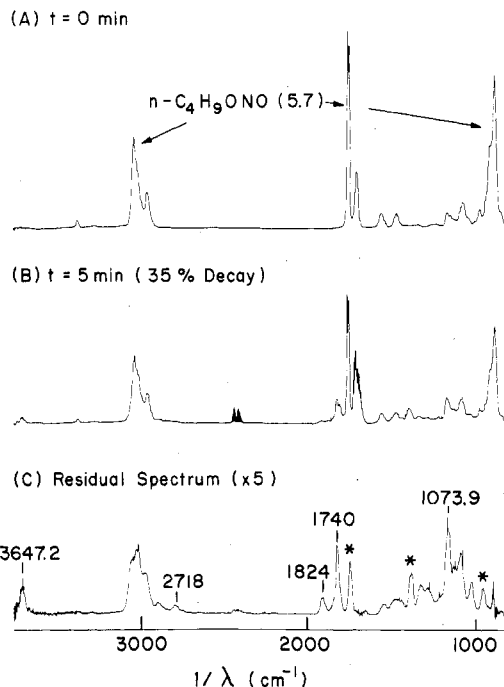


Figure 2. Photolysis of $n\text{-C}_4\text{H}_9\text{ONO}$ (5.7 ppm) in 1 torr of O₂ and 700 torr of N₂: (A) before irradiation, (B) after 5 min irradiation, and (C) residual spectrum from (B) (see text). The absorbance scale for (C) was expanded by a factor of 5 as compared with those for (A) and (B).

Some cursory attempts were made to characterize the unknown products formed in this system. Illustrated in Figure 2 are the spectral data obtained from the photolysis of $n\text{-C}_4\text{H}_9\text{ONO}$ (5.7 ppm) in 1 torr of O₂ and 700 torr of N₂. The low O₂ pressure used in this run was intended to make reaction 1 dominant over reaction 2 and yet sufficient to sustain reaction 4. The residual spectrum shown in Figure 2C is a result of spectral subtraction of all the identified products. This residual spectrum suggests the presence of several functional groups, i.e., HO (3647.2 cm⁻¹), CHO (2718 cm⁻¹), C=O (1824, 1750 cm⁻¹), OONO₂ (1740 cm⁻¹), and C(O)OH (1050, 1100 cm⁻¹). Many of these broad bands appear to consist of at least two contributing bands. The three bands indicated by asterisks in this figure correspond to "nitrate (ONO₂)-type" compounds formed during aging of the unknown products in the dark. In addition several sharp peaks centered at 978.8, 1073.9, and 1181.1 cm⁻¹ are present. The relative intensity distribution among the various absorption bands changed somewhat depending on the particular experimental conditions used. However (with the possible exception of the C=O band at about 1820 cm⁻¹), these spectral variations were not sufficiently distinct to permit the desynthesis of this composite residual spectrum into individual components. Nevertheless, the intense bands corresponding to O–H stretching (~3650 cm⁻¹) and C–OH stretching (1000–1100 cm⁻¹) modes provide conclusive evidence for the occurrence of isomerization, reaction 1. Baldwin et al.³ and Carter et al.⁴ suggested several possible subsequent reactions for the CH₂(OH)CH₂CH₂CH₂O₂ radicals and the corresponding HO-containing products, e.g., HOCH₂CH₂CH₂CHO, CH(OH)₂CH₂CHO, HOC(O)CH₂CHO, and (HO)₂CO. However, residual spectra such as Figure 2C alone do not allow unique distinction among all these possible products and their nitrates. Further work is underway to generate reference spectra needed for such positive identification.

(8) J. R. Barker, S. W. Benson, and D. M. Golden, *Int. J. Chem. Kinet.*, **9**, 31 (1977).

(9) L. Batt, *NBS Spec. Publ.*, U.S., No. 557, 62 (1979).